

# Hands-on exercises: 6-field 2-fluid model



**Tianyang Xia<sup>1,2</sup>, X.Q. Xu<sup>2</sup> and BOUT++ team**

<sup>1</sup>Institute of Plasma Physics, Chinese Academy of Sciences, Hefei, China.

<sup>2</sup>Lawrence Livermore National Laboratory, Livermore, CA 94550, USA

**2018 BOUT++ mini workshop  
August 14<sup>th</sup>-17<sup>th</sup>, 2018**





- Introduction of 6-field 2-fluid model
  - Equations & boundary conditions
  - Physics switches
  - Edge turbulence simulations of H-mode on EAST
  - Summary for divertor simulations
- Demo for running 6-field



- Introduction of 6-field 2-fluid model
- Applications for divertor simulations
  - Transient heat flux simulations during ELM bursts on DIII-D
    - ◆ Kinetic modification on thermal conduction in pedestal
    - ◆ Validation with experiments
    - ◆ Study on the effects of magnetic flutter in parallel conduction
  - Transient particle flux simulations during ELM bursts on EAST
  - Summary for divertor simulations
- Demo for running 6-field



Six-field two-fluid model is necessary to describe:

- pedestal energy loss
- density profile evolution through the ELM event,
- heat flux
- energy depositions on divertor target
- Edge turbulence

Six-field ( $\varpi$ ,  $n_i$ ,  $T_i$ ,  $T_e$ ,  $A_{||}$ ,  $V_{||}$ ): based on Braginskii equations, the density, momentum and energy of ions and electrons are described in drift ordering[1,2].

---

[1]X. Q. Xu et al., *Commun. Comput. Phys.* **4**, 949 (2008).

[2]T. Y. Xia et al., *Nucl. Fusion* **53**, 073009 (2013).



# Equations of 6-field 2-fluid model



$$\frac{\partial}{\partial t} \varpi = -\frac{1}{B_0} \mathbf{b} \times \nabla_{\perp} \Phi \cdot \nabla \varpi + B_0^2 \nabla_{\parallel} \left( \frac{J_{\parallel}}{B_0} \right) + 2\mathbf{b} \times \boldsymbol{\kappa} \cdot \nabla p_i$$

$$- \frac{1}{2\Omega_i} \left[ \frac{1}{B_0} \mathbf{b} \times \nabla P_i \cdot \nabla (\nabla_{\perp}^2 \Phi) - Z_i e B_0 \mathbf{b} \times \nabla n_i \cdot \nabla \left( \frac{\nabla_{\perp} \Phi}{B_0} \right)^2 \right]$$

$$+ \frac{1}{2\Omega_i} \left[ \frac{1}{B_0} \mathbf{b} \times \nabla \Phi \cdot \nabla (\nabla_{\perp}^2 P_i) - \nabla_{\perp}^2 \left( \frac{1}{B_0} \mathbf{b} \times \nabla \Phi \cdot \nabla P_i \right) \right] + \mu_{\parallel i} \nabla_{\parallel 0}^2 \varpi, \quad (1)$$

$$\frac{\partial}{\partial t} n_i = -\frac{1}{B_0} \mathbf{b} \times \nabla_{\perp} \Phi \cdot \nabla n_i - \frac{2n_i}{B_0} \mathbf{b} \times \boldsymbol{\kappa} \cdot \nabla \Phi$$

$$- \frac{2}{Z_i e B_0} \mathbf{b} \times \boldsymbol{\kappa} \cdot \nabla P_i - n_i B_0 \nabla_{\parallel} \left( \frac{V_{\parallel i}}{B_0} \right), \quad (2)$$

$$\frac{\partial}{\partial t} V_{\parallel i} = -\frac{1}{B_0} \mathbf{b} \times \nabla_{\perp} \Phi \cdot \nabla V_{\parallel i} - \frac{1}{m_i n_{i0}} \mathbf{b} \cdot \nabla P, \quad (3)$$

$$\frac{\partial}{\partial t} A_{\parallel} = -\nabla_{\parallel} \phi + \frac{\eta}{\mu_0} \nabla_{\perp}^2 A_{\parallel} + \frac{1}{e n_{e0} B_0} \nabla_{\parallel} P_e + \frac{0.71 k_B}{e B_0} \nabla_{\parallel} T_e - \frac{\eta H}{\mu_0} \nabla_{\perp}^4 A_{\parallel}, \quad (4)$$

$$\frac{\partial}{\partial t} T_i = -\frac{1}{B_0} \mathbf{b} \times \nabla_{\perp} \Phi \cdot \nabla T_i$$

$$- \frac{2}{3} T_i \left[ \left( \frac{2}{B_0} \mathbf{b} \times \boldsymbol{\kappa} \right) \cdot \left( \nabla \Phi + \frac{1}{Z_i e n_{i0}} \nabla P_i + \frac{5}{2} \frac{k_B}{Z_i e} \nabla T_i \right) + B_0 \nabla_{\parallel} \left( \frac{V_{\parallel i}}{B_0} \right) \right]$$

$$+ \frac{2}{3 n_{i0} k_B} \nabla_{\parallel 0} (\kappa_{\parallel i} \nabla_{\parallel 0} T_i) + \frac{2}{3 n_{i0} k_B} \nabla_{\perp} \cdot (\kappa_{\perp i} \nabla_{\perp} T_i) + \frac{2 m_e Z_i}{m_i \tau_e} (T_e - T_i), \quad (5)$$

$$\frac{\partial}{\partial t} T_e = -\frac{1}{B_0} \mathbf{b} \times \nabla_{\perp} \Phi \cdot \nabla T_e$$

$$- \frac{2}{3} T_e \left[ \left( \frac{2}{B_0} \mathbf{b} \times \boldsymbol{\kappa} \right) \cdot \left( \nabla \Phi - \frac{1}{e n_{e0}} \nabla P_e - \frac{5}{2} \frac{k_B}{e} \nabla T_e \right) + B_0 \nabla_{\parallel} \left( \frac{V_{\parallel e}}{B_0} \right) \right]$$

$$+ 0.71 \frac{2 T_e}{3 e n_{e0}} B_0 \nabla_{\parallel} \left( \frac{J_{\parallel}}{B_0} \right) + \frac{2}{3 n_{e0} k_B} \nabla_{\parallel 0} (\kappa_{\parallel e} \nabla_{\parallel 0} T_e) + \frac{2}{3 n_{e0} k_B} \nabla_{\perp} \cdot (\kappa_{\perp e} \nabla_{\perp} T_e)$$

$$- \frac{2 m_e}{m_i} \frac{1}{\tau_e} (T_e - T_i) + \frac{2}{3 n_{e0} k_B} \eta_{\parallel} J_{\parallel}^2, \quad (6)$$

Compressible terms
Parallel velocity terms
Electron Hall
Thermal force
Gyro-viscosity
Energy exchange
Energy flux
Thermal conduction



# Boundary conditions and normalizations



Boundary conditions:

Inner boundary:

$$\partial n_i / \partial \Psi = 0, \partial T_j / \partial \Psi = 0, \varpi = 0, \nabla_{\perp}^2 A_{\parallel} = 0, \partial^2 \phi / \partial^2 \Psi = 0, \partial V_{\parallel} / \partial \Psi = 0$$

Outer boundary:

$$n_i = 0, T_j = 0, \varpi = 0, \nabla_{\perp}^2 A_{\parallel} = 0, \partial^2 \phi / \partial^2 \Psi = 0, V_{\parallel} = 0$$

Sheath boundary conditions on the divertors

Normalizations:

$$\begin{aligned} \hat{T}_j &= \frac{T_j}{\bar{T}_j}, & \hat{n} &= \frac{n_i}{\bar{n}}, & \hat{L} &= \frac{L}{\bar{L}}, \\ \hat{t} &= \frac{t}{\bar{t}}, & \hat{B} &= \frac{B}{\bar{B}}, & \hat{J} &= \frac{\mu_0 \bar{L}}{B_0} J, \\ \hat{\psi} &= \frac{\psi}{\bar{L}}, & \hat{\phi} &= \frac{\bar{t}}{L^2 B_0} \phi, & \hat{\varpi} &= \frac{\bar{t}}{m_i \bar{n}} \varpi, \\ \tau &= \frac{\bar{T}_i}{\bar{T}_e}, & \hat{V} &= \frac{V}{V_A}, & V_A &= \frac{\bar{L}}{\bar{t}} = \frac{\bar{B}}{\sqrt{\mu_0 m_i n_i}}, \\ \hat{P}_j &= \frac{P_j}{k_B \bar{n} \bar{T}_j}, & \hat{\kappa} &= \bar{L} \kappa, & \hat{\nabla} &= \bar{L} \nabla \end{aligned}$$



# The physics switches of 6-field model in BOUT++



Switch Name	Physics meanings
compress0	Parallel velocity
continuity	Compressible terms
eHall	Electron Hall effects
energy_flux	Energy flux terms
energy_exch	Energy exchange terms
thermal_force	Thermal force terms
gyro_viscous	Gyro-viscosity
viscos_par	Parallel viscosity
spitzer_resist	Spitzer resistivity
hyperresist	Hyper resistivity
diffusion_par	Thermal conduction
experimental_Er	Using diagnostic Er
Neoclassic_i/e	Neoclassical transport for ion/electron
Gamma_i/e_BC	Sheath boundary for ion/electron



# 3-field 2-fluid model is good enough to simulate P-B stability and ELM crashes, additional physics from multi-field contributes less than 25% corrections



## Fundamental physics in ELMs:

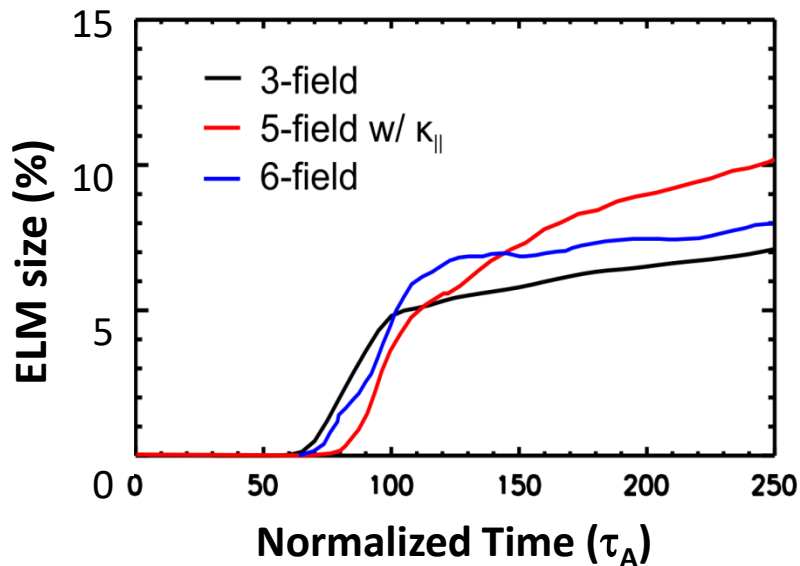
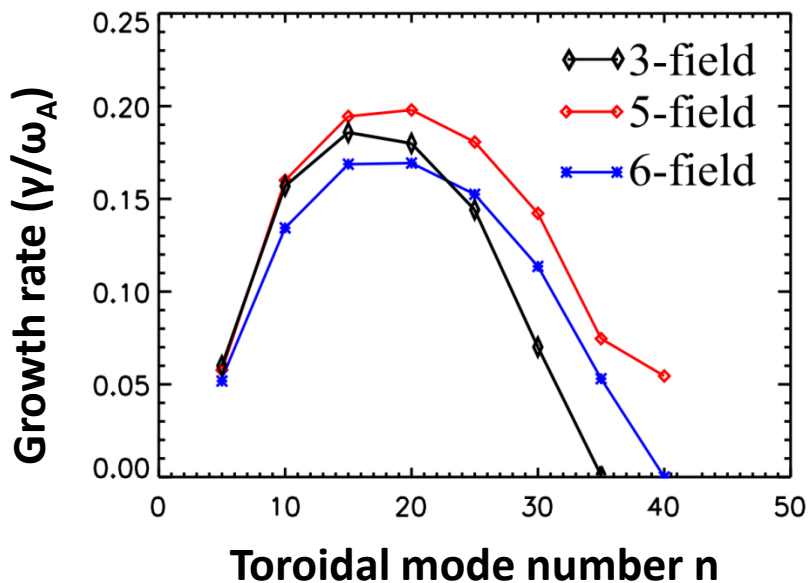
- ✓ Peeling-Ballooning instability
- ✓ Ion diamagnetic stabilization
  - kinetic effect
- ✓ Resistivity and hyper-resistivity
  - reconnection

## Additional physics:

- Ion acoustic waves
- Thermal conductivities
- Hall effect
- Compressibility
- Electron-ion friction

change the linear growth rate less than **25%**

Power depositions on PFCs.  
Turbulence and transport



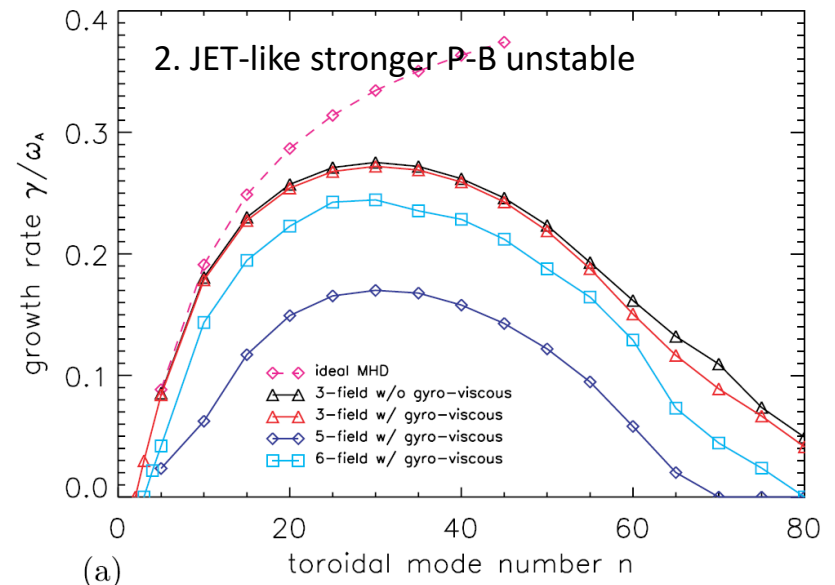
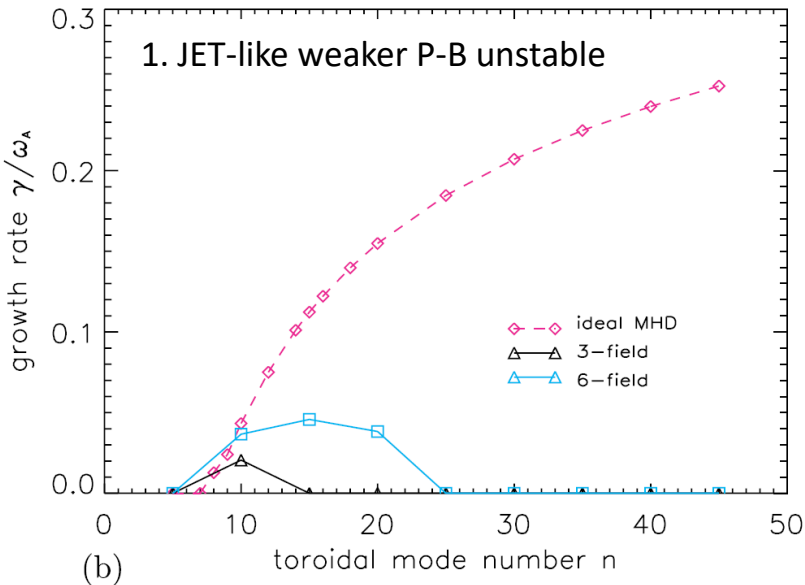
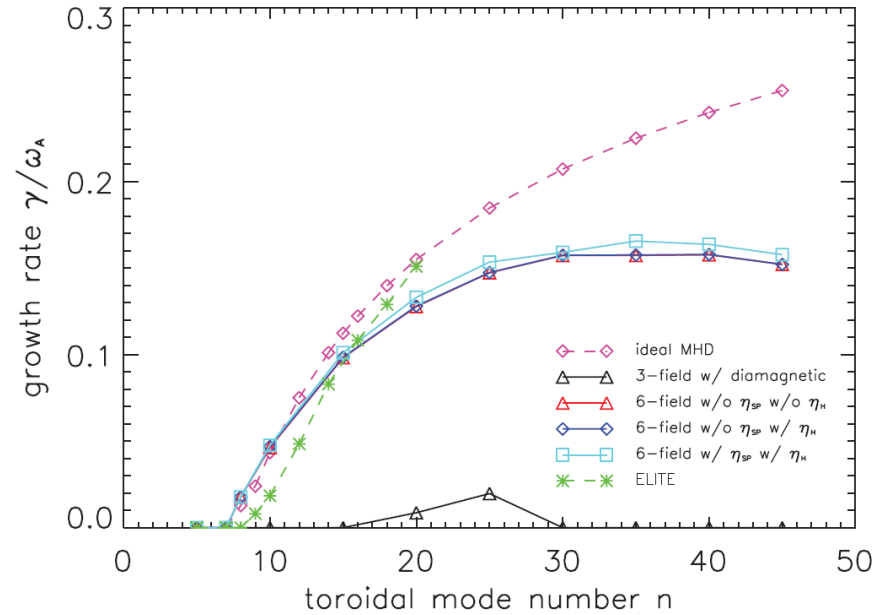


# Benchmark with ELITE and 3-field mode in BOUT++



For a typical peeling-ballooning mode unstable equilibrium:

- Ideal MHD, the growth rate is consistent with ELITE.
- Full 6-field mode gives smaller growthrate than ideal MHD, mostly due to FLR effects.
- Higher than 3-field model w/ diamagnetic effects, most due to electromagnetic drift wave instability





# Flux limiting coefficients describe the kinetic modification to Spitzer-Harm-Braginskii thermal conduction



$$\kappa_{\parallel i} = 3.9 n_i v_{th,i}^2 / \nu_i \quad \kappa_{\parallel e} = 3.2 n_e v_{th,e}^2 / \nu_e$$

$$\kappa_{fs,j} = n_j v_{th,j} q R_0 \alpha_j$$

$$\kappa_{eff,j} = \frac{\kappa_{\parallel j} \kappa_{fs,j}}{\kappa_{\parallel j} + \kappa_{fs,j}}$$

Flux limiting coefficient  $\alpha_j$  represents the ratio of the Spitzer-Harm-Braginskii expression for parallel heat flux vs. free streaming flux.

The typical range of  $\alpha_j$  is [0.03, 3.0]\*

How to determine the value of  $\alpha_j$ :

The free streaming limit:  $\alpha_j^{FS} = 0.8 - 1.0$

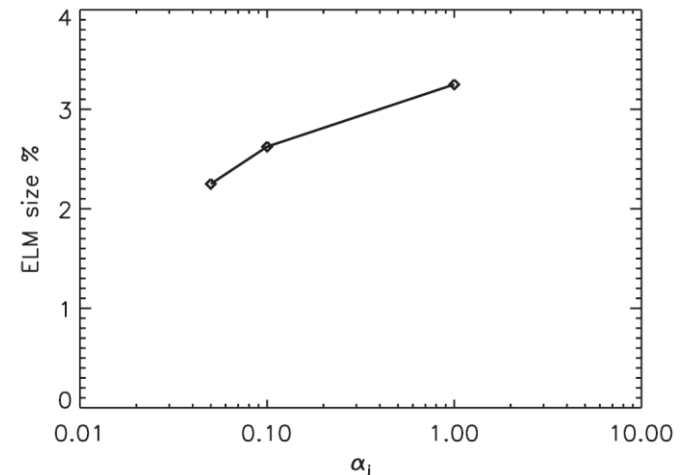
The sheath limit:  $\alpha_j^{SH} \simeq 2.5 \left( \frac{T_i}{T_e} + Z_i \right)^{\frac{1}{2}} \left( \frac{m_e}{m_i} \right)^{\frac{1}{2}} \simeq 0.058$   
 -- should be chosen for divertor simulations

For DIII-D #144382,  $\kappa_{\parallel j}$  are dominated by the flux limited expression because of low collisionality, especially inside the separatrix.

$v_{e^*} = 0.127$  at  $\psi_N = 0.8$

$v_{e^*} = 1.616$  at pressure gradient peak

The simulated ELM size under sheath limit parallel conduction with  $\alpha_i = 0.05$  is around **2.2%**, which is very close to the experimental measurement with **2%\*\***.



\* P.W. Fundamenski, Plasma Phys. Controlled Fusion 47, R163 (2005).

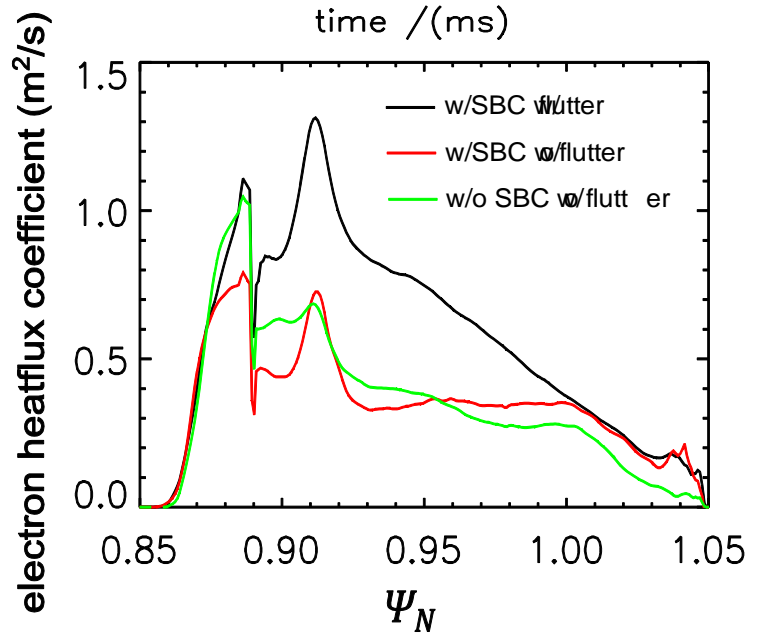
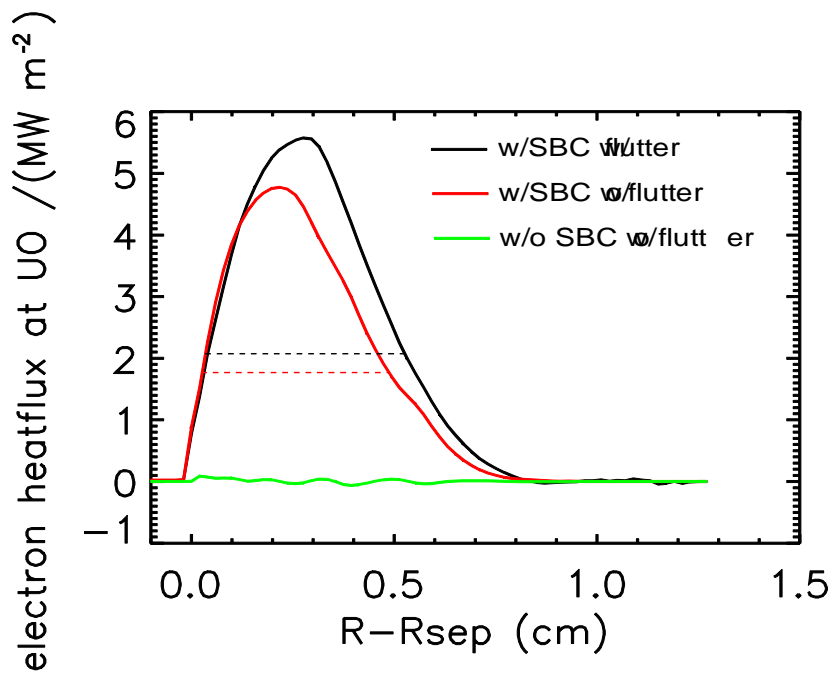
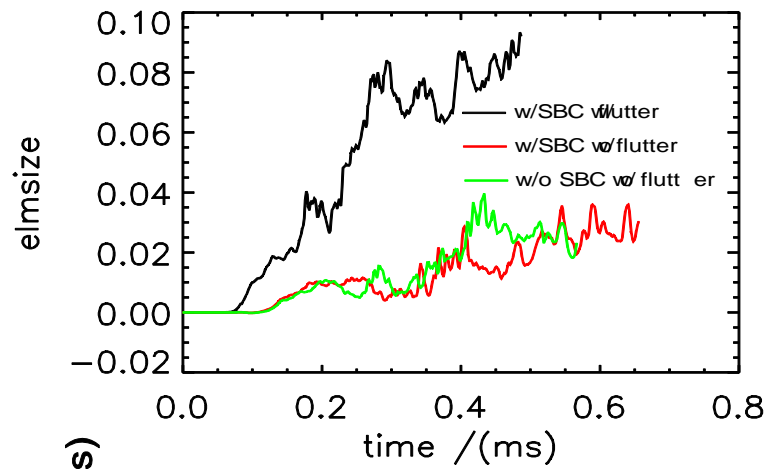
\*\* M.E.Fenstermacher, et al. 40th EPS Conference on Plasma Physics, P4.104.



# The magnetic flutter enhance radial transport, then leads to larger Energy loss and heat flux



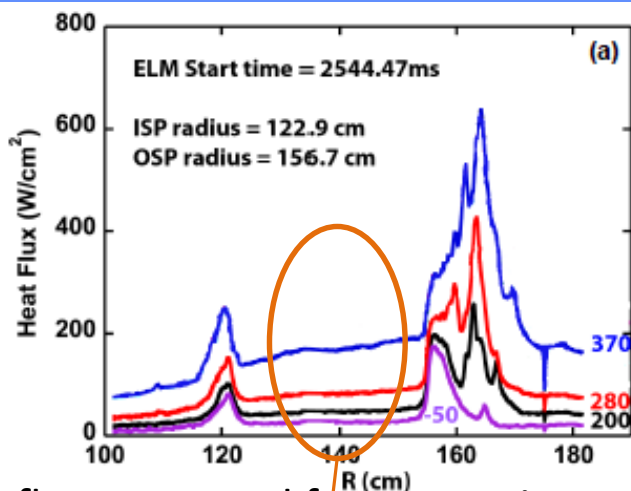
- More energy loss is due to magnetic flutter.
- SBCs slightly increase the ELM size
- At the linear phase, the growing of the perturbation is enhanced by flutter



- Wider spreading of heat flux to targets, but larger peak value by flutter.
- Radial transport is enhanced by flutter. SBCs does not change it obviously.

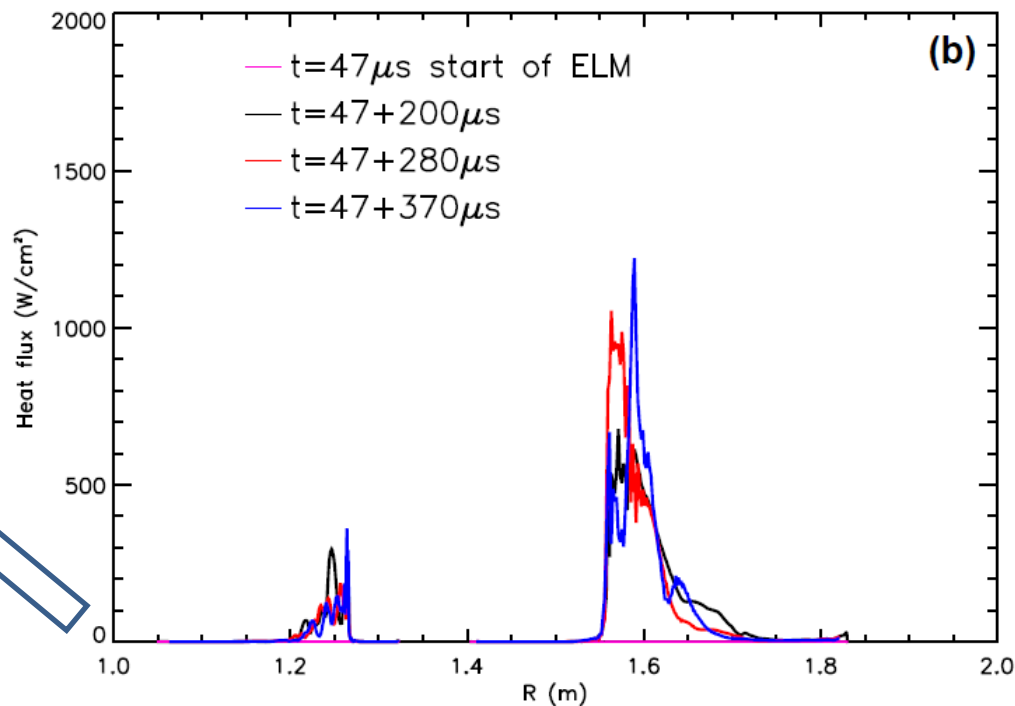


# The comparison of the heat flux profiles between simulations and measurements on DIII-D



Heat flux measured from experiments\*.

Due to reflections in the IRTV, which have been significantly reduced in the 2013 DIII-D campaign.



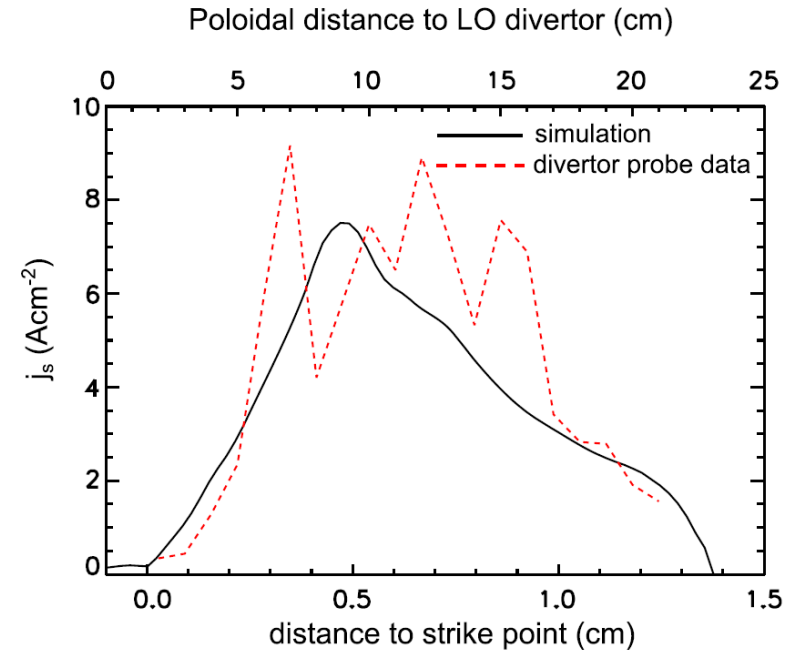
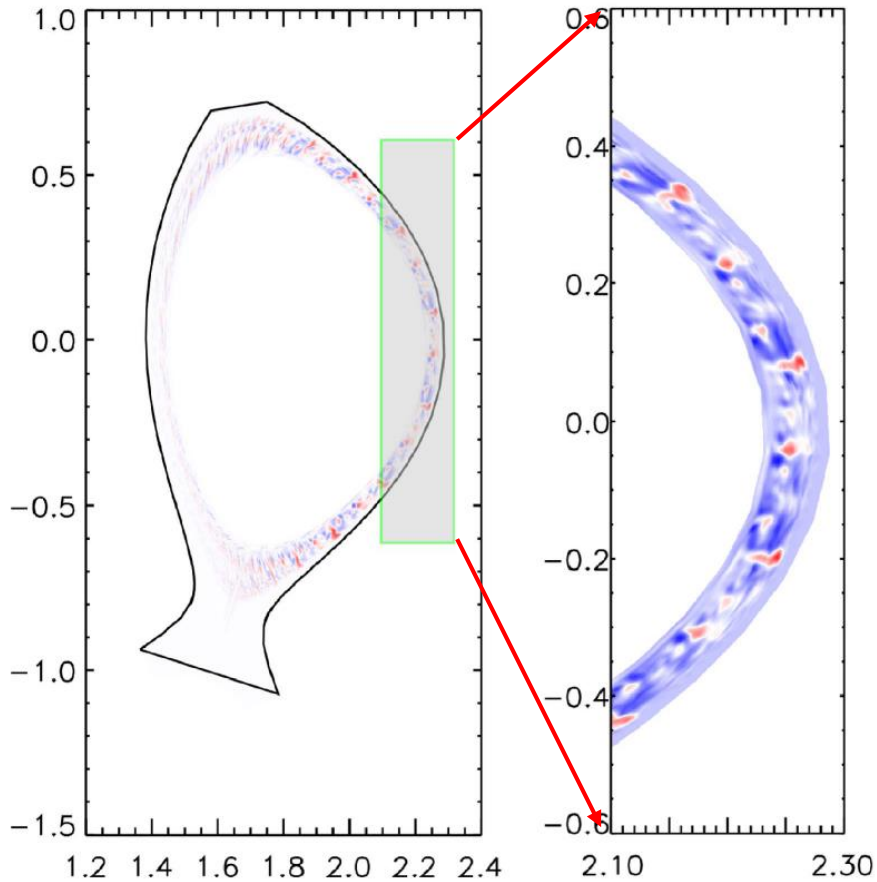
- Heat fluxes from simulations show the comparable expansion on targets.
- Compared to the measurement, the amplitude is 2x times larger due to the lack of radiation and recombination by neutrals and impurities.



# The validations between BOUT++ and EAST experiments are also well agreed



➤ The blob transport behavior is obtained



- The BOUT++ simulations shows the similar amplitude and depositions with divertor probes.
- The width is a little narrow because of LHW.



- Introduction of 6-field 2-fluid model
  - Equations & boundary conditions
  - Physics switches
  - Edge turbulence simulations of H-mode on EAST
  - Summary for divertor simulations
- Demo for running 6-field



# The physics switches used for this hands-on exercise



Switch Name	Physics meanings
compress0	Parallel velocity
continuity	Compressible terms
eHall	Electron Hall effects
energy_flux	Energy flux terms
energy_exch	Energy exchange terms
thermal_force	Thermal force terms
gyro_viscous	Gyro-viscosity
viscos_par	Parallel viscosity
spitzer_resist	Spitzer resistivity
hyperresist	Hyper-resistivity
diffusion_par	Thermal conduction
experimental_Er	Using diagnostic Er
Neoclassic_i/e	Neoclassical transport for ion/electron
Gamma_i/e_BC	Sheath boundary for ion/electron



# Density profile as the input



Density profile used in 6-field model:

$$n_{i0}(x) = \frac{(n_{\text{height}} \times n_{\text{ped}})}{2} \left[ 1 - \tanh \left( \frac{x - x_{\text{ped}}}{\Delta x_{\text{ped}}} \right) \right] + n_{\text{ave}} \times n_{\text{ped}},$$

The coefficients in BOUT.inp:

```
[highbeta]
#hyperbolic tanh profile, N0 = N0tanh(n0_height*Nbar, n0_ave*Nbar, n0_width, n0_center)
n0_fake_prof = true      #use the hyperbolic profile of n0. If both n0_fake_prof and T0_fake_prof
n0_height = 0.           #the total height of profile of N0, in percentage of Ni_x
n0_ave = 0.2             #the constant tail of N0 profile, in percentage of Ni_x
n0_width = 0.1          #the width of the gradient of N0, in percentage of x
n0_center = 0.633       #the the center of N0, in percentage of x
n0_bottom_x = 0.81      #the start of flat region of N0 on SOL side, in percentage of x
```



# Compiling and running of 6-field module



For the exercise, a simple linear test is prepared:

Compiling:

> vi makefile

```
SOURCEC      = elm_6f.cxx
```

```
-> = 6f_landau.cxx
```

> make

Go to the scratch directory to run the code:

> cd \$SCRATCH

> cd -r ~/BOUT++/merge-github/examples/6f\_landau/ .

> cp ~/BOUT++/merge-github/examples/6f\_landau/6field-simple/\* .

> cp \$SCRATCH/Transport\_Code/code/job\_submit\_job.sh .

Submit job and run the job:

➤ vi job\_submit.sh

```
srun -n 64 ./trans_er_Nn -d data
```

```
-> srun -n 64 ./6f_landau -d data
```

➤ sbatch submit\_job.sh

DCJP	FLOAT	= Array[68, 64, 101]
DCNI	FLOAT	= Array[68, 64, 101]
DCP	FLOAT	= Array[68, 64, 101]
DCPH	FLOAT	= Array[68, 64, 101]
DCPS	FLOAT	= Array[68, 64, 101]
DCTE	FLOAT	= Array[68, 64, 101]
DCTI	FLOAT	= Array[68, 64, 101]
DCU	FLOAT	= Array[68, 64, 101]
DCVP	FLOAT	= Array[68, 64, 101]
G	STRUCT	= -> <Anonymous> Array[1]
GR	FLOAT	= Array[1, 1, 101]
JP	FLOAT	= Array[68, 64, 16, 101]
NI	FLOAT	= Array[68, 64, 16, 101]
P	FLOAT	= Array[68, 64, 16, 101]
PH	FLOAT	= Array[68, 64, 16, 101]
PS	FLOAT	= Array[68, 64, 16, 101]
PSN	DOUBLE	= Array[68]
RMSJP	FLOAT	= Array[68, 64, 101]
RMSNI	FLOAT	= Array[68, 64, 101]
RMSP	FLOAT	= Array[68, 64, 101]
RMSPH	FLOAT	= Array[68, 64, 101]
RMSPS	FLOAT	= Array[68, 64, 101]
RMSTE	FLOAT	= Array[68, 64, 101]
RMSTI	FLOAT	= Array[68, 64, 101]
RMSU	FLOAT	= Array[68, 64, 101]
RMSVP	FLOAT	= Array[68, 64, 101]
TE	FLOAT	= Array[68, 64, 16, 101]
TI	FLOAT	= Array[68, 64, 16, 101]
U	FLOAT	= Array[68, 64, 16, 101]
VP	FLOAT	= Array[68, 64, 16, 101]

Variables after the collecting

Data post-processing:

Add the idl library directory first

```
IDL> !path=!path+":$BOUT_TOP/tools/idllib"
```

```
IDL> @collect-all
```

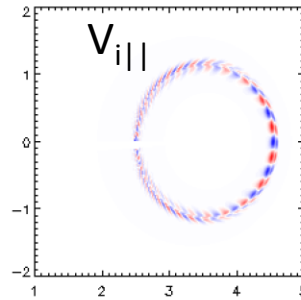
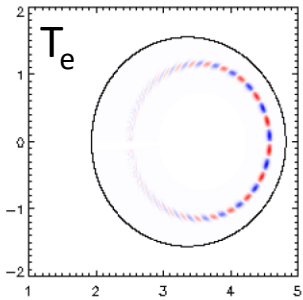
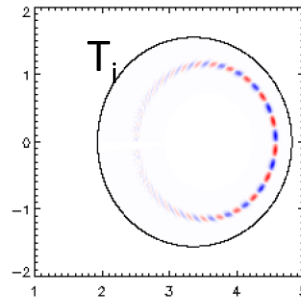
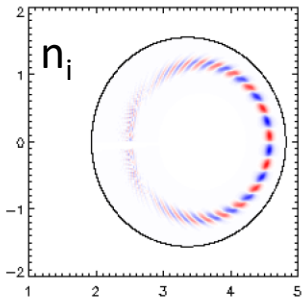


## ➤ Download the transport code

```
$ cd $SCRATCH/  
$ cp -r ~train38/PUBLIC/BOUT++_Workshop_2018/Transport_Code ./  
$ cd Transport_Code/code
```



# The output of the mode structure (1)



Poloidal mode structures

>cp BOUT.inp data/.

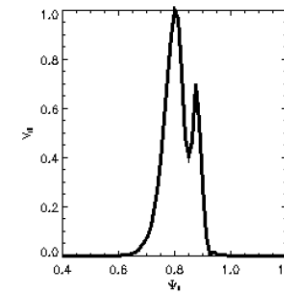
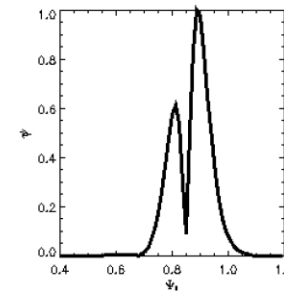
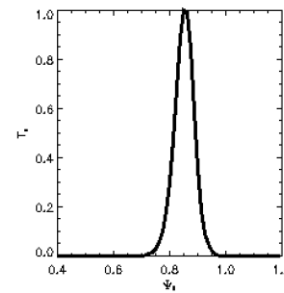
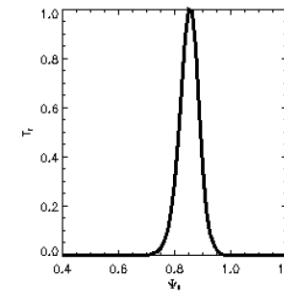
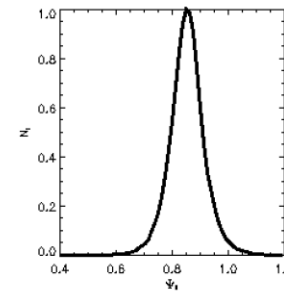
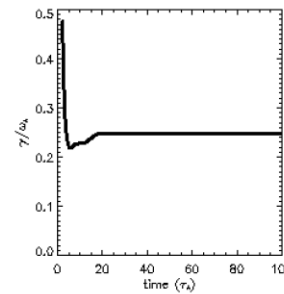
n0\_height = 0.0

n0\_ave = 2

Linear growth rate for this test case:

IDL> print,gr[-1]

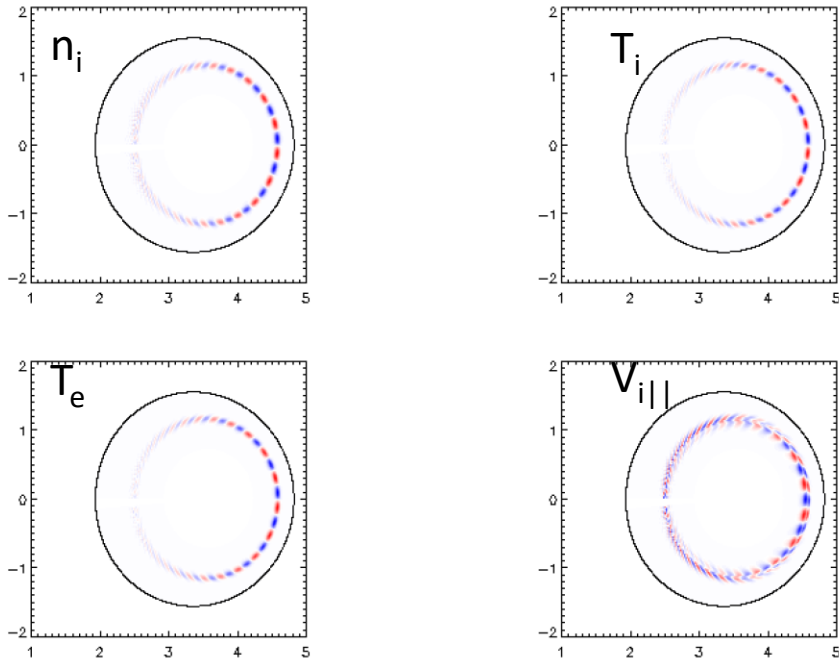
0.248578



Linear growth rate and radial mode structures



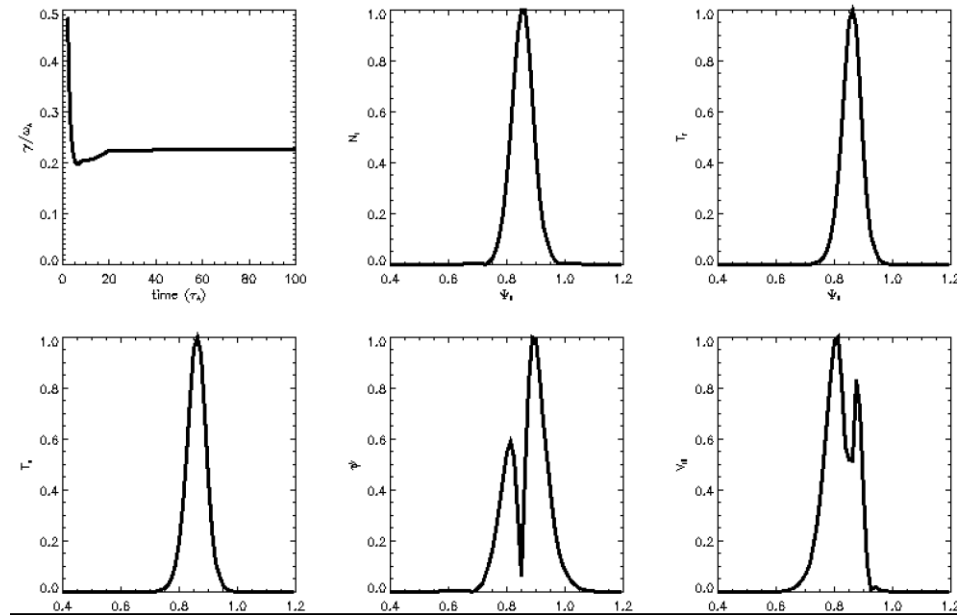
# The output of the mode structure (3)



Poloidal mode structures

$n0\_height = 0.9$   
 $n0\_ave = 2$

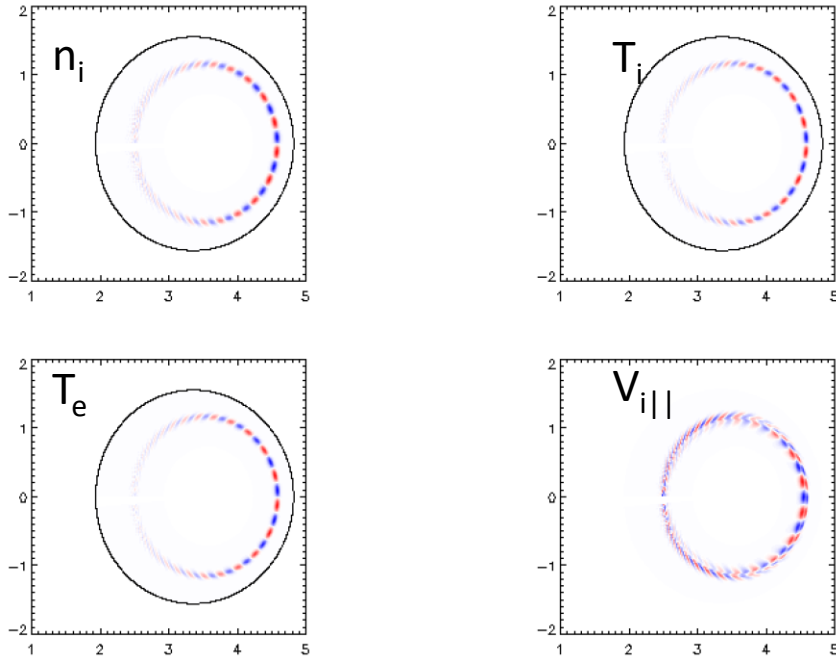
Linear growth rate for this test case:  
`IDL> print,gr[-1]`  
**0.226131**



Linear growth rate and radial mode structures



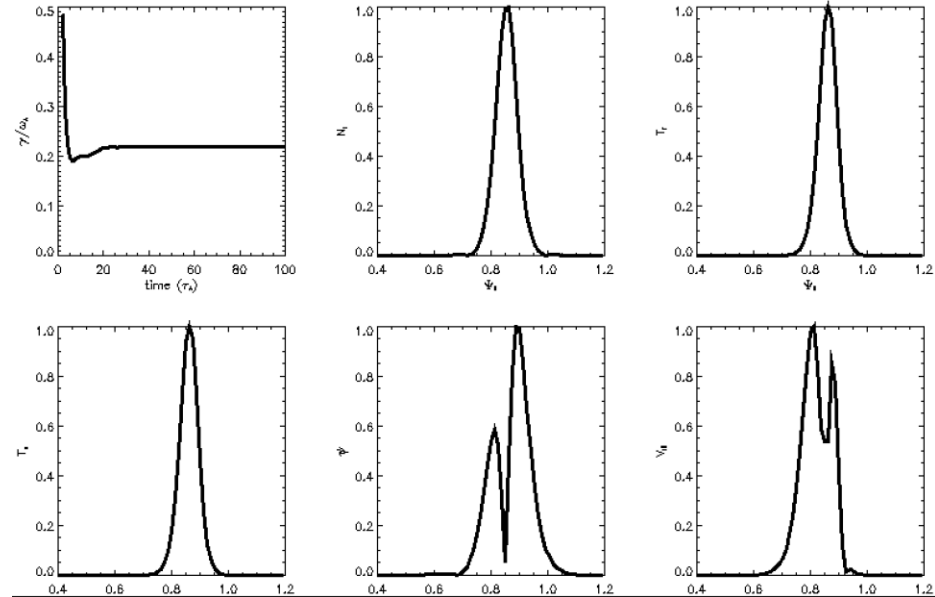
# The output of the mode structure (2)



Poloidal mode structures

$n0\_height = 1.2$   
 $n0\_ave = 2$

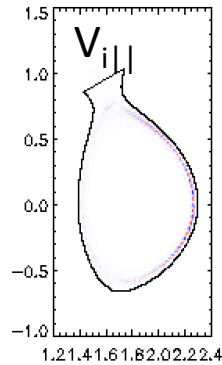
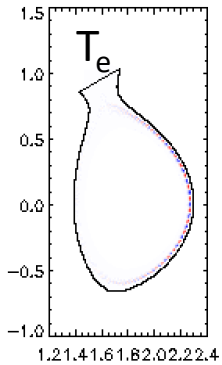
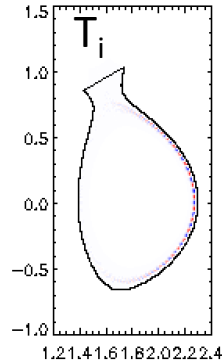
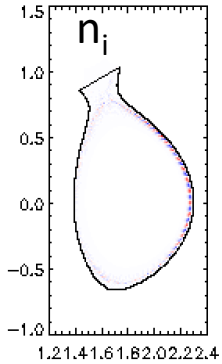
Linear growth rate for this test case:  
`IDL> print,gr[-1]`  
 0.219981



Linear growth rate and radial mode structures



# Examples for an X-point geometry



Poloidal mode structures

cp \$BOUT\_TOP/examples/6f\_landau/6field-simple/east077741.03500\_psi080to105\_x260y64.nc .

In BOUT.inp  
grid="east077741.03500\_psi080to105\_x260y64.nc"

**NXPE = 4**

n0\_height = 0.0

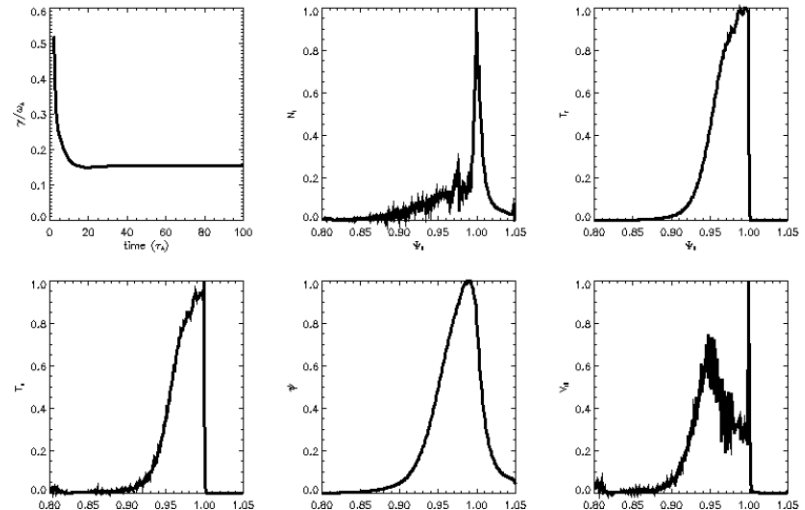
n0\_ave = 0.2

Linear growth rate for this test case:

IDL> print,gr[-1]

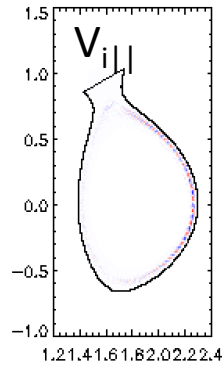
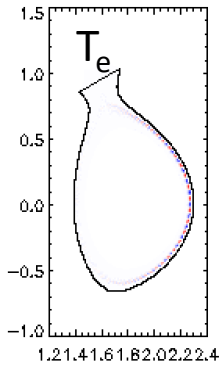
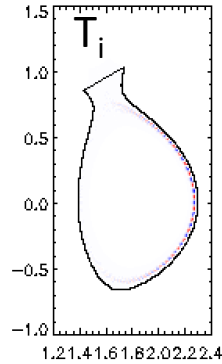
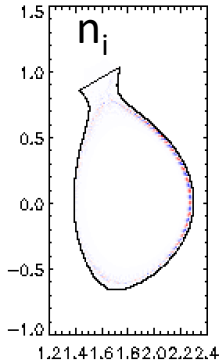
0.154437

Linear growth rate and radial mode structures





# Examples for an X-point geometry



Poloidal mode structures

In BOUT.inp

```
grid="east077741.03500_psi080to105_x260y64.nc"
```

**NXPE = 4**

n0\_height = 0.0

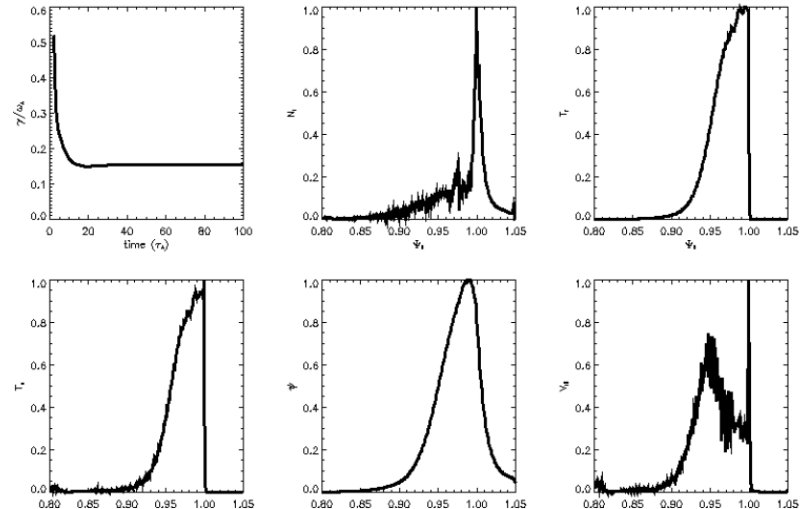
n0\_ave = 0.2

Linear growth rate for this test case:

```
IDL> print,gr[-1]
```

0.154437

Linear growth rate and radial mode structures



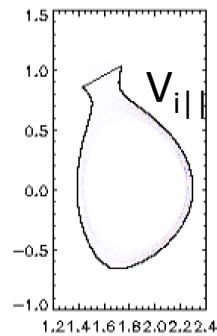
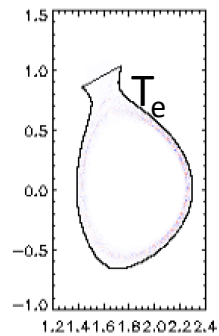
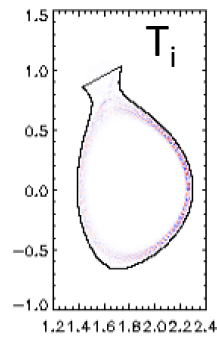
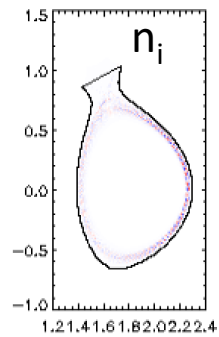


# Backup slides





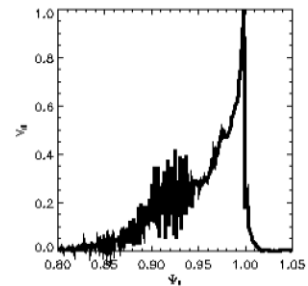
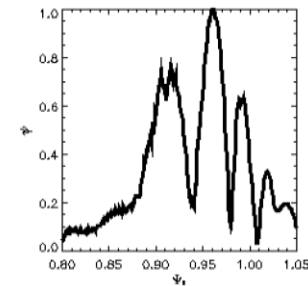
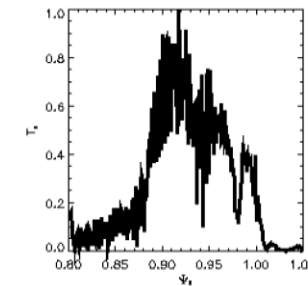
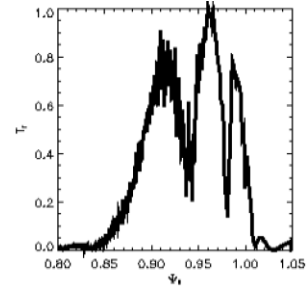
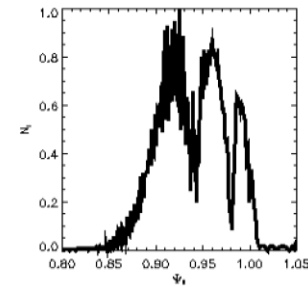
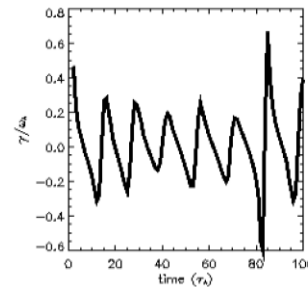
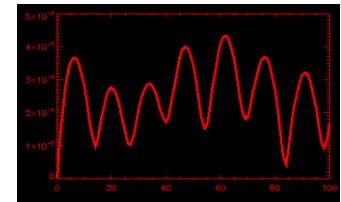
# Examples with measured density profiles



In BOUT.inp  
n0\_fake\_prof = **false**

Linear growth rate for this test case:  
IDL> plot,rmsp[xx,yy,\*]

The mode does not grow!



Poloidal mode structures

Linear growth rate and radial mode structures



# The background impurity can be taken into account in order to use full set of measured



The vorticity equation with background impurity is modified to

$$\begin{aligned} \frac{\partial}{\partial t} \varpi &= - \left( \frac{1}{B_0} \mathbf{b} \times \nabla_{\perp} \Phi + V_{\parallel i} \mathbf{b} \right) \cdot \nabla \varpi + B^2 \nabla_{\parallel} \left( \frac{J_{\parallel}}{B} \right) + 2 \mathbf{b} \times \boldsymbol{\kappa} \cdot \nabla p_1 \\ &\quad - \frac{1}{2\Omega_i} \left[ \frac{1}{B} \mathbf{b} \times \nabla P_i \cdot \nabla (\nabla_{\perp}^2 \Phi) - Z_i e B \mathbf{b} \times \nabla n_i \cdot \nabla \left( \frac{\nabla_{\perp} \Phi}{B} \right)^2 \right] \\ &\quad + \frac{1}{2\Omega_i} \left[ \frac{1}{B} \mathbf{b} \times \nabla \Phi \cdot \nabla (\nabla_{\perp}^2 P_i) - \nabla_{\perp}^2 \left( \frac{1}{B} \mathbf{b} \times \nabla \Phi \cdot \nabla P_i \right) \right] \\ &\quad - \frac{1}{2\Omega_{im}} [n_{im} Z_{im} e V_{Dim} \cdot \nabla (\nabla_{\perp}^2 \Phi) - m_{im} \Omega_{im} \mathbf{b} \times \nabla n_{im} \cdot \nabla V_E^2] \\ &\quad + \frac{1}{2\Omega_{im}} [V_E \cdot \nabla (\nabla_{\perp}^2 P_{im}) - \nabla_{\perp}^2 (V_E \cdot \nabla P_{im})]. \end{aligned}$$

Gyro-viscous

$$\begin{aligned} \varpi &= \mathbf{b} \cdot \nabla \times (m_i n_i V_i + m_{im} n_{im} V_{im}) \\ &\simeq n_{i0} \frac{m_i}{B_0} \left( \nabla_{\perp}^2 \phi + \frac{1}{n_{i0}} \nabla_{\perp} \phi \cdot \nabla_{\perp} n_{i0} + \frac{1}{n_{i0} Z_i e} \nabla_{\perp}^2 p_{i1} \right) \\ &\quad + n_{im} \frac{m_{im}}{B_0} \left( \nabla_{\perp}^2 \phi + \frac{1}{n_{im}} \nabla_{\perp} \phi \cdot \nabla_{\perp} n_{im} \right). \end{aligned}$$

Quasi-neutral condition

$$Z_i n_{i0} + Z_{im} n_{im} = n_{e0}$$

$$n_j = n_{j0} + n_{j1},$$

$$P_j = P_{j0} + p_{j1},$$

$$P = P_i + P_e + P_{im} = P_0 + p_1 = (P_{i0} + P_{e0}) + (p_{i1} + p_{e1}) + P_{im},$$

$$\Phi = \Phi_0 + \phi,$$

$$J_{\parallel} = J_{\parallel 0} + J_{\parallel 1},$$

$$V_{\parallel e} = \frac{Z_i n_i}{n_e} V_{\parallel i} - \frac{J_{\parallel 1}}{en_e},$$

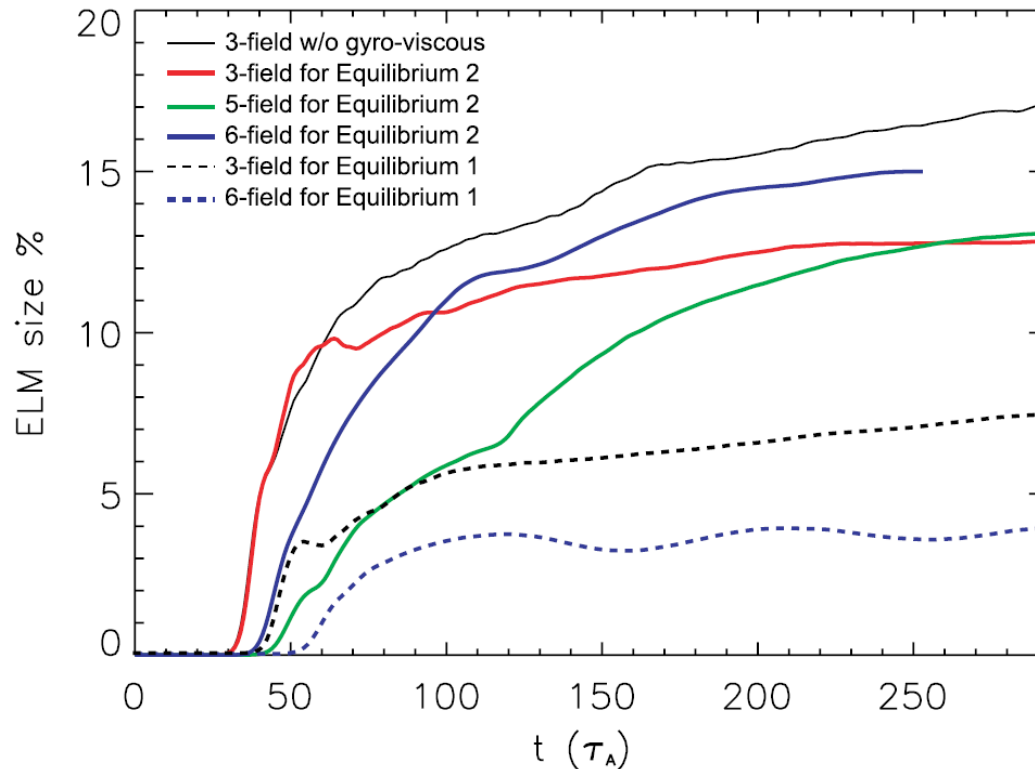
$$\mathbf{b} = \mathbf{b}_0 - \mathbf{b}_0 \times \nabla \psi,$$

$$J_{\parallel 1} = -\frac{1}{\mu_0} B_0 \nabla_{\perp}^2 \psi.$$

The effects of impurity: all the terms are at the order of  $m_{im} n_{im}$



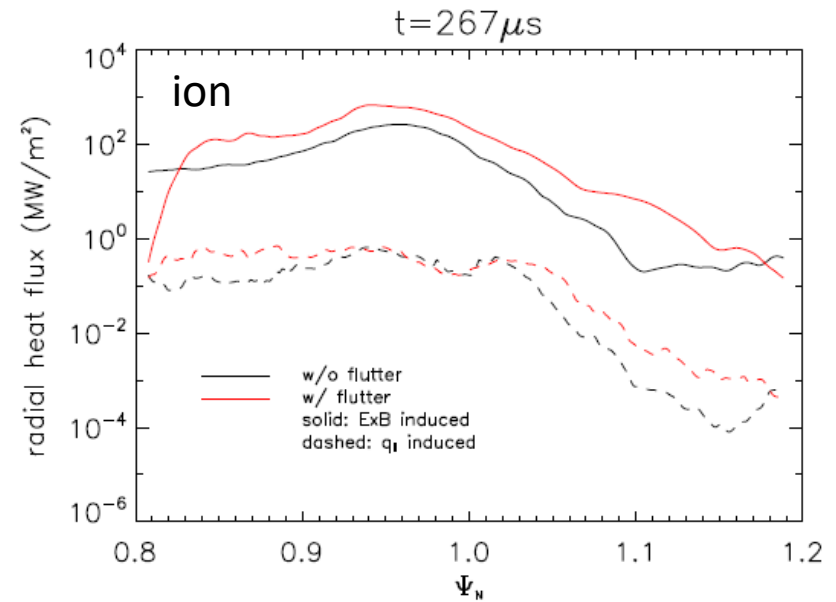
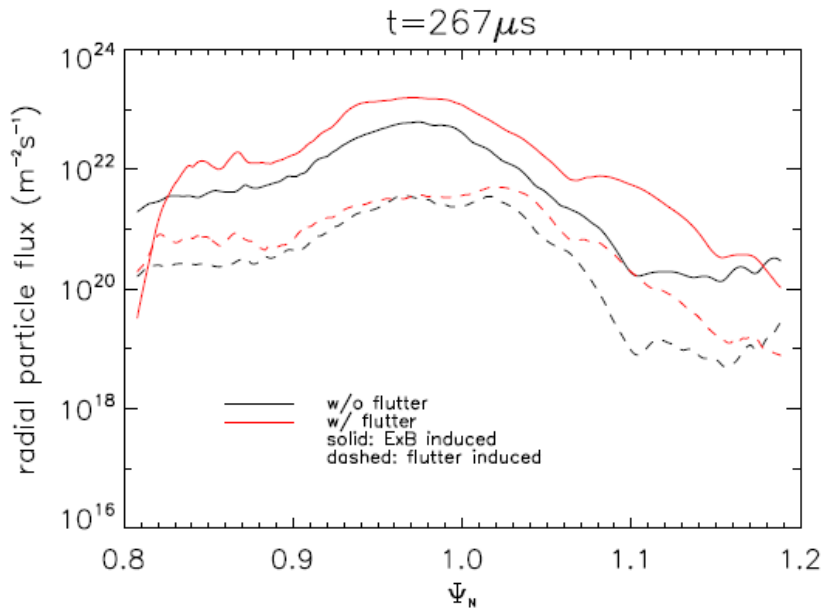
# Nonlinear comparison with 3-field model



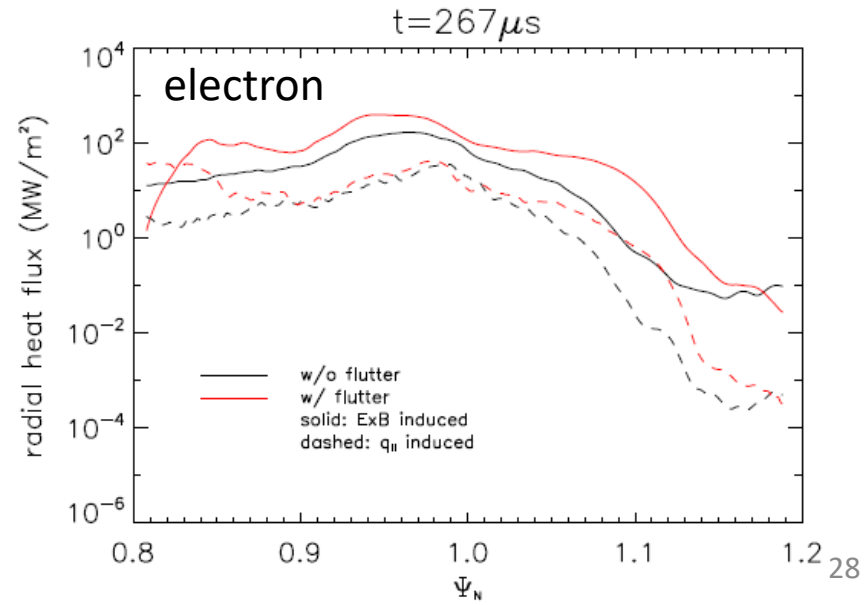
- For weaker P-B unstable equilibrium (1), both three-field and six-field models show the consistent results at linear and nonlinear phases.
- In stronger P-B unstable equilibrium (2), while additional terms of six-field do enhance the instability.
- The six-field model yields smaller ELM size than 3-field model in both equilibria.



# The magnetic flutter enhance radial transport



- Radial particle flux and heat fluxes are all enhanced by magnetic flutter
- More effective on ion heat flux than electron.
- The effects of magnetic flutter are mainly on the ExB induced fluxes
- The non-consistent calculation of conductive fluxes are similar to the consistent one, especially near the separatrix.





# Simulations show the filaments of ELMs and heat load strips on targets

